Low-temperature saturation of phase coherence length in topological insulators

Saurav Islam,[1,*] Semonti Bhattacharyya,[1,2] Hariharan Nhalil,[1] Mitali Banerjee,[1,3] Anthony Richardella,[4] Abhinav Kandala,[4,5] Diptiman Sen,[6] Nitin Samarth,[4] Suja Elizabeth,[1] and Arindam Ghosh[1,7]

[1]*Department of Physics, Indian Institute of Science, Bangalore, 560012 India*
[2]*School of Physics and Astronomy, Monash University, VIC 3800, Australia*
[3]*Department of Physics, Columbia University, New York, New York 10027, USA*
[4]*Department of Physics, The Pennsylvania State University, University Park, Pennsylvania 16802-6300, USA*
[5]*IBM T.J. Watson Research Center, Yorktown Heights, New York 10598, USA*
[6]*Center for High Energy Physics, Indian Institute of Science, Bangalore, 560012 India*
[7]*Center for Nanoscience and Engineering, Indian Institute of Science, Bangalore, 560012 India*

(Received 20 March 2019; published 13 June 2019)

Implementing topological insulators as elementary units in quantum technologies requires a comprehensive understanding of the dephasing mechanisms governing the surface carriers in these materials, which impose a practical limit to the applicability of these materials in such technologies requiring phase coherent transport. To investigate this, we have performed magnetoresistance (MR) and conductance fluctuations (CF) measurements in both exfoliated and molecular beam epitaxy grown samples. The phase breaking length (l_ϕ) obtained from MR shows a saturation below sample dependent characteristic temperatures, consistent with that obtained from CF measurements. We have systematically eliminated several factors that may lead to such behavior of l_ϕ in the context of TIs, such as finite size effect, thermalization, spin-orbit coupling length, spin-flip scattering, and surface-bulk coupling. Our work indicates the need to identify an alternative source of dephasing that dominates at low T in topological insulators, causing saturation in the phase breaking length and time.

DOI: 10.1103/PhysRevB.99.245407

I. INTRODUCTION

Topological insulators (TIs) [1–4] are a new class of materials characterized by the presence of gapless and linearly dispersing metallic surface states which lie in the bulk band gap due to a nontrivial topology of the bulk band structure. The surface carriers are prohibited from backscattering against nonmagnetic impurities and exhibit a plethora of fundamentally important effects such as spin-momentum locking, hosting Majorana fermions in the presence of a superconductor, topological magnetoelectric effect, quantum anomalous Hall effect, and also can be used in optoelectronic devices [1,5,6]. The topological protection of these surface states makes these materials a strong contender for the building blocks of qubits, which requires long phase coherence length (l_ϕ) for error tolerant quantum computation. Hence, it is critical to understand the mechanisms responsible for dephasing or decoherence, which is equivalent to loss of information, in the surface states of TIs. The most common dephasing mechanism in TIs at low temperature (T) has been known to be electron-electron interaction [7–11], and the coupling of the surface states to localized charged puddles in the bulk [12]. Li *et al.* have demonstrated that electron-phonon interaction is also required to explain the dependence of l_ϕ on T [13]. Although theoretically, all these mechanisms lead to a diverging l_ϕ with decreasing T [7,8,14,15], experimentally, the increase of l_ϕ with reducing T is often followed by its saturation below sample specific temperatures [12,13,16,17]. The saturation of l_ϕ at a finite value instead of its divergence for $T \to 0$ K, which is predicted for electron-electron or electron-phonon interactions, has been a matter of active discourse [15,18–29].

In this report, we have inspected the factors that can lead to the saturation of l_ϕ in TIs by measuring both gate-voltage (V_G) and time (t)-dependent conductance fluctuations and magnetoresistance (MR) [28,30–37]. Conductance fluctuations result from the quantum interference of different electron trajectories, manifested as sample specific, aperiodic fluctuations in the conductance due to varying disorder configuration, Fermi energy, and magnetic field; such fluctuations have been used as a tool to probe the presence of time-reversal symmetry (TRS) breaking disorders, since the saturation of l_ϕ at low T is often attributed to spin-flip scattering processes. The magnitude of the conductance fluctuations $\langle \delta G^2 \rangle$, however, shows a factor of two reduction upon application of a perpendicular magnetic field ($B_\perp$), implying that TRS is intrinsically preserved in these systems. Additionally, at different gate voltages, $\langle \delta G^2 \rangle$ displays a saturation for $T < 2$ K, even in the presence of a large $B_\perp$ which suppresses spin-spin scattering; this implies that neither magnetic impurities nor the coupling of the surface and the bulk impurity states is responsible for the saturation. Our experiment suggests an unconventional mechanism that saturates l_ϕ in TIs, possibly arising from unscreened Coulomb fluctuations from the charged disorders present in the bulk [12].

II. EXPERIMENTAL RESULTS

The field effect devices investigated in this paper were fabricated from both exfoliated and molecular beam epitaxy

*isaurav@iisc.ac.in

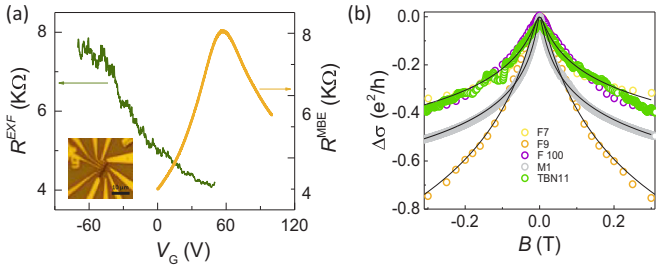

FIG. 1. Quantum transport in topological insulator FETs. (a) Typical $R - V_G$ for exfoliated TI (R^{EXF}) TBN11 and epitaxially grown TI (R^{MBE}) M10 at 20 mK. Inset: optical micrograph of a typical exfoliated TI FET. (b) Weak-antilocalization behavior observed in different samples at $T = 300$ mK. The solid black lines are fits to the data using Eq. (1).

(MBE) grown TIs. To fabricate the former, the TI $Bi_{1.6}Sb_{.4}Te_2Se$ (BSTS) (purity of the starting elements Bi, Te, Sb, Se $\geqslant$ 4N) was exfoliated from a single crystal onto a $SiO_2/Si++$ substrate with the 285 nm thick SiO_2 acting as the back gate dielectric [38]. This was followed by standard electron-beam lithography and sputtering of 100 nm Au to form the source-drain contacts [inset of Fig. 1(a)]. The details of the devices measured are provided in Table I. The samples F7, F100, F9, and TBN11 were exfoliated from the same bulk single crystal on SiO_2/Si. In sample TBN11, the TI flake was transferred onto an atomically flat boron nitride (BN) substrate to reduce the effect of charged traps and dangling bonds of SiO_2 on the electrical transport [39], followed by lithography and metallization. The quarternary alloy BSTS offers a reduced bulk number density due to compensation doping, resulting in a higher percentage of surface transport [38]. The exfoliated samples were covered with PMMA [poly(methylmethacrylate)] during the entire measurement cycle to prevent oxidation and subsequent degradation of the surface quality. The large area (0.5 mm × 1 mm) sample (M10) was fabricated from thin (thickness, $d = 10$ nm) $(Bi, Sb)_2Te_3$ (BST) (purity of starting elements was 5N for Bi, 5N for Sb, and 6N for Te), grown by molecular beam epitaxy (MBE) on the ⟨111⟩ $SrTiO_3$ (STO) substrate and mechanically etched into Hall bars with a metallic coating of indium at the back, that was used as a back gate electrode [40,41]. Resistivity measurements were performed in a low-frequency four-probe AC configuration in a pumped He-3 system (base $T = 320$ mK) and in a dilution refrigerator (base $T = 20$ mK).

Preliminary electrical transport characteristics in the exfoliated device TBN11 (at $T = 20$ mK) and the MBE-grown device (at 20 mK) are shown in Fig. 1(a). The R-V_G data indicates that at $V_G = 0$ V, TBN11 is intrinsically electron doped and M10 is intrinsically hole doped. Whereas M10 shows a clear graphene like ambipolar transport with a Dirac point at 60 V, which could be achieved due to the high dielectric constant of the STO at low T ($\epsilon_r \sim 44000$ at 5 K) [41], TBN11 shows a clear signature of electron-hole puddle regime at $V_G = -60$ V. The estimated value of intrinsic number density at $V_G = 0$ V are -2.9×10^{13} m^{-2} and 9×10^{13} m^{-2}, respectively. The quantitative difference of the V_G-dependent characteristics here indicates dominance of different types of disorder species in the samples, owing to different processes of synthesis, fabrication, and composition. The n-doping in BSTS mostly comes due to Se vacancies, the most probable cause of p doping in the epitaxially grown samples is the presence of antisite defects. The R vs T of the exfoliated samples display metallic to semiconducting behavior, depending on their thickness (d), and for $d < 1$ μm, and $T < 50$ K, the exfoliated samples display 100% surface transport [42]. The MBE-grown sample shows metallic behavior due to the dominance of surface states [41].

Figure 1(b) shows weak antilocalization (WAL) for different samples, which is characterized by a cusp in the quantum correction to conductivity $\triangle\sigma$ at $B = 0$ T and is a result of π Berry phase in topological insulators. The magnetoconductance data can be fitted with the Hikami-Larkin-Nagaoka (HLN) expression for diffusive metals with high spin-orbit coupling ($\tau_\phi \gg \tau_{so}, \tau_e$) [30,43–45]:

$$\triangle\sigma = -\alpha\frac{e^2}{\pi h}\left[\psi\left(\frac{1}{2}+\frac{B_\phi}{B}\right) - \ln\left(\frac{B_\phi}{B}\right)\right], \qquad (1)$$

where τ_ϕ, τ_{so}, and τ_e are the phase coherence or dephasing time, spin-orbit scattering time, and elastic scattering time, respectively, ψ is the digamma function, and B_ϕ is the phase breaking field. Here α and B_ϕ are fitting parameters. The phase coherence length l_ϕ^{MR} can be extracted using $l_\phi^{MR} = \sqrt{\hbar/4eB_\phi}$ and the value of α gives an estimate of the number of independent conducting channels in the sample (see Supplemental Material [46]).

The magnitude of gate voltage dependent conductance fluctuations $\langle\delta G^2\rangle$ has been evaluated by using a method similar to Refs. [17,36,47] by varying the chemical potential with the back gate voltage in steps of 5 mV over a small window of 4 V. $\langle\delta R^2\rangle$ is extracted from R-V_G by fitting the data with a smooth polynomial curve. $\langle\delta G^2\rangle$ is

TABLE I. Details of measured devices: The thickness, substrate, composition, saturation value of temperature (T^{sat}), and saturation value of phase breaking length (l_ϕ^{sat}) for various devices that have been investigated are provided in the table.

Sample	Thickness	Substrate	Composition	T^{sat}	l_ϕ^{sat}
F7	7	$SiO_2/Si++$	$Bi_{1.6}Sb_{.4}Te_2Se$	∼2 K	200 nm
F100	100	$SiO_2/Si++$	$Bi_{1.6}Sb_{.4}Te_2Se$	∼2 K	150 nm
F9	9	$SiO_2/Si++$	$Bi_{1.6}Sb_{.4}Te_2Se$	∼2 K	NA
TBN11	11	Boron nitride	$Bi_{1.6}Sb_{.4}Te_2Se$	∼2 K	190 nm
M10	10	STO	$(Bi, Sb)_2Te_3$	∼300 mK	2000 nm

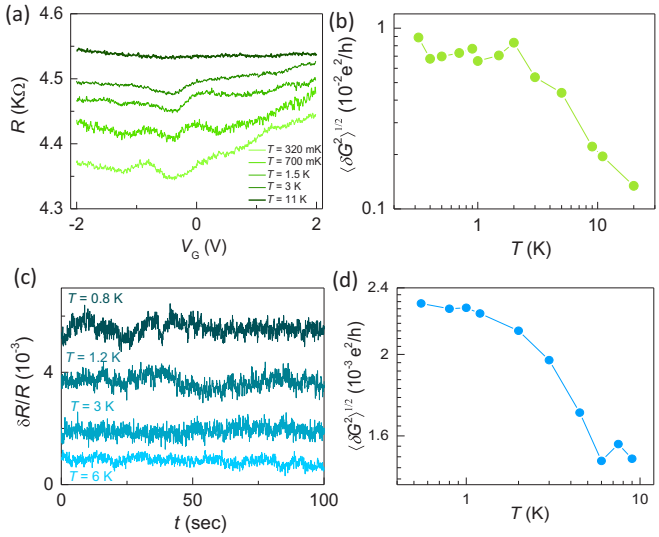

FIG. 2. Conductance fluctuations measurements F100. (a) R vs V_G for different T for device F100 in a 4 V window, used to extract $\langle\delta G^2\rangle$. (b) $\langle\delta G^2\rangle^{1/2}$ as a function of T which shows a saturation below $T < 2$ K for the device F100. Above 2 K, $\langle\delta G^2\rangle^{1/2} \propto 1/T^{0.5}$. (c) Normalized resistance fluctuations in the time domain for different T used for calculation of P.S.D in device F100. (d) Noise magnitude as a function of T also showing a saturation below $T < 2$ K. Above 2 K, $\langle\delta G^2\rangle^{1/2} \propto 1/T^{0.5}$.

then obtained using the relation: $\langle\delta G^2\rangle = \langle\delta R^2\rangle/\langle R\rangle^4$ ($\langle\delta R^2\rangle$ is extracted from the variance of the residual). As shown in Fig. 2(a) for a typical 4 V window, the fluctuations are aperiodic yet reproducible but weaken with increasing T. The T dependence of the standard deviation $\langle\delta G^2\rangle^{\frac{1}{2}}$, at $V_G = 0$ V (center of the corresponding window) for F100 in Fig. 2(b) shows two distinctly different regions. Above $T > 2$ K, $\langle\delta G^2\rangle^{\frac{1}{2}} \propto T^{-0.5}$, which is expected from the T dependence of $l_\phi \propto T^{-0.5}$ and the number of active scatterers ($n_s \propto T$). $\langle\delta G^2\rangle^{\frac{1}{2}}$, however, saturates for $T < 2$ K.

Conductance fluctuations due to changes in the disorder configuration were detected by measuring the normalized noise magnitude, defined as $\frac{\langle\delta G^2\rangle}{\langle G^2\rangle} = \frac{\int S_V df}{V^2}$ where S_V/V^2 is the normalized power spectral density (P.S.D.) of the time-dependent signal, in an AC-four probe Wheatstone bridge technique ([33,48]). The normalized time-dependent fluctuations in resistance, $(\delta R/R)$ for various temperatures ($0.3\ \text{K} \leqslant T \leqslant 6$ K) is shown in Fig. 2(c). $\langle\delta G^2\rangle^{\frac{1}{2}}$ extracted from the P.S.D. of time-dependent conductance fluctuations is plotted as a function of T in Fig. 2(d) and is found to show a saturation below $T = 2$ K, which is consistent with the behavior of $\langle\delta G^2\rangle^{\frac{1}{2}}$ obtained from the V_G dependence. The order of magnitude difference is caused due to integration of the signal over a finite frequency window as well as the sensitivity of resistance changes to individual defect movements [37,49–51].

The phase breaking length l_ϕ extracted from $\langle\delta G^2\rangle^{\frac{1}{2}}$-$T$ data [Fig. 2(b)] using the expression [52,53]

$$\langle\delta G^2\rangle \simeq \left(\frac{3}{\pi}\right)\left(\frac{e^2}{h}\right)^2\left(\frac{l_\phi}{L}\right)^2 \tag{2}$$

is shown in Fig. 3(a). Since $\langle\delta G^2\rangle \propto l_\phi^2$, any saturation obtained from time or gate voltage dependence should also be reflected in the saturation of l_ϕ, obtained directly from MR measurements. The values of l_ϕ extracted from MR data similar to Fig. 1(b), as a function of T for the exfoliated samples F100 and F7, is shown in Fig. 3(b). We find that l_ϕ obtained from two different methods, l_ϕ^{MR} and l_ϕ^{UCF} [extracted from Eq. (1) and Eq. (2), respectively) show similar trends with T, first increasing with decreasing T, followed by a saturation below $T \sim 2$ K, thus discarding the possibility of the saturation to be an artifact. The discrepancies in the values of l_ϕ^{MR} and l_ϕ^{UCF} are within uncertainties of the prefactor of Eq. (2) [52–54]. The saturation of l_ϕ obtained from three different methods (t- and V_G-dependent conductance fluctuations and MR) on the same sample F100 validates our measurements and analysis. The higher value of l_ϕ for F7 compared to $F100$ can be due to enhanced dephasing due to trapping-detrapping processes in the bulk, since the thickness of F100 is much larger than that of F7 or due to different surface-bulk coupling. Similar saturation of l_ϕ in both F7 and F100 also eliminates

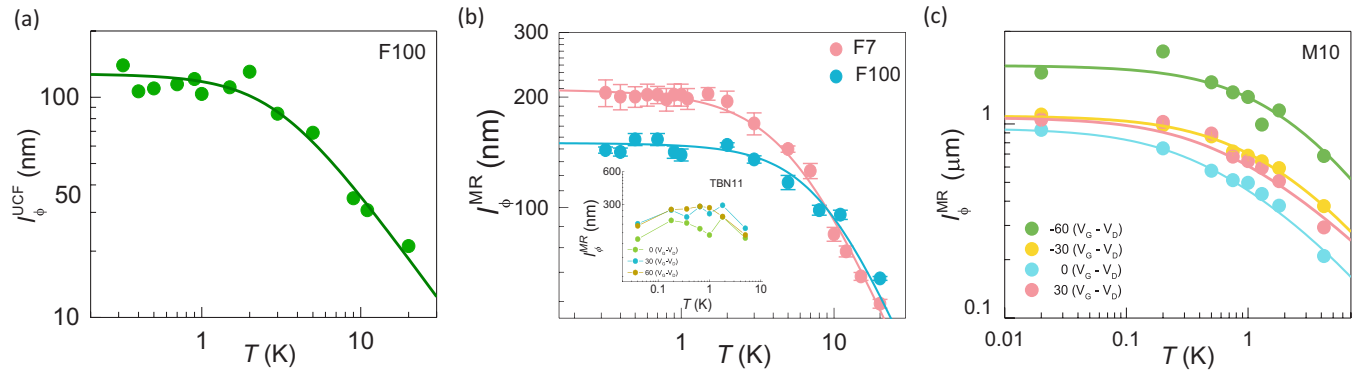

FIG. 3. Saturation of phase breaking length (l_ϕ). (a) l_ϕ vs T extracted from T dependence of $\langle\delta G^2\rangle$ using Eq. (2) for device F100. The solid line is fit according to Eq. (4). (b) l_ϕ vs T extracted from T dependence of WAL data using Eq. (1) for exfoliated samples F7 and F100 which shows a saturation below $T < 2$ K. The solid lines are fits to Eq. (1). Inset shows l_ϕ vs T extracted from T dependence of WAL data for sample TBN11, which also shows a saturation. (c) l_ϕ vs T for different V_G extracted from T dependence of WAL data using Eq. (1) for epitaxially grown TI M10 which shows a saturation below $T < 300$ mK. The solid lines are fits to Eq. (3).

the coupling between bulk and surface states to be the source of the saturation.

For a quantitative understanding, l_ϕ-T data [Figs. 3(a) and 3(b)] has been fitted with the expression commonly used to fit the l_ϕ-T data in 2D diffusive systems [13,15].

$$l_\phi = \frac{1}{(A_0 + A_1 T + A_2 T^2)^{0.5}} \tag{3}$$

Here, $l_\phi \propto T^{-0.5}$ and $l_\phi \propto T^{-1}$ are the respective contributions from electron-electron (e-e) and electron-phonon (e-ph) scattering. A_1, A_2 are fitting parameters and $A_0 = \frac{1}{l_{\phi 0}^2}$ is the saturation value of l_ϕ. In 2D systems, although e-e interactions are the dominant source of dephasing at low T and have been adequate to describe dephasing in graphene [15,55,56], and in some reports of TIs [14,57], e-ph interaction cannot be neglected for TIs because of the vicinity of the bulk to the surface states [12,13]. However, instead of saturation, these two mechanisms lead to a diverging l_ϕ at low T. The saturation of l_ϕ has also been obtained in device TBN11, where the TI has been transferred onto a boron nitride substrate for different $V_G - V_D$, in both the bulk and surface dominated regime [Fig. 3(b)]. The atomically flat boron nitride (thickness $d =$ 14 nm) also prevents trapping-detrapping that is commonly observed between the channel and the SiO_2 substrate, thus reducing any dephasing due to electromagnetic fluctuations induced by potential traps present in SiO_2.

The saturation of l_ϕ is often attributed to (a) finite size effects, where l_ϕ becomes comparable to L, the length of the sample, (b) saturation of electron temperature due to heating from external sources [15], (c) spin-orbit scattering length becoming comparable to the phase breaking length [18], and (d) magnetic impurities or local magnetic moment [23,25,26]. We have systematically explored the possibility of saturation arising from any of the above reasons. To probe the effect of finite size, we have performed MR measurements on M10 with a channel length of 1 mm which is three orders of magnitude more than the saturated value of l_ϕ. The l_ϕ extracted from magnetoconductance data using Eq. (1) also shows a saturation for $T < 300$ mK for all $(V_G - V_D)$, irrespective of bulk or surface dominated regime [Fig. 3(c)]. The saturation obtained in the large area sample M10 indicates that finite-size effects at low T is not the cause of the observed behavior of l_ϕ. We also note that the temperature where l_ϕ saturates in M10 is ~300 mK, which is an order of magnitude lower compared to the exfoliated samples (F7, F10, and TBN11), and $l_\phi^{\rm sat}$ is also an order of magnitude higher. This difference in $l_\phi^{\rm sat}$ and $T^{\rm sat}$ between these samples, grown by totally different methods could be indicative of a lower charge impurity driven inhomogeneity in the bulk in the case of the MBE sample. The saturation of l_ϕ obtained in both exfoliated samples and thin films, in both surface and bulk-dominated regimes, although at different temperatures, indicates the universality of the effect in topological insulators. Another important factor for the saturation is thermalization, where the electron T_e can be much higher than the lattice temperature T_L. For extracting T_e accurately in our He-3 system, we have measured and analyzed the T dependence of Shubnikov-de Haas oscillations using $GaAs/Al_{0:33}Ga_{0:66}As$ heterostructure to ensure that down to $T = 0.3$ K, T_e matches T_L. This type of saturation has also been observed in systems where the spin-orbit coupling length (l_{SO}) becomes comparable to the phase breaking length [18]. We have extracted l_{SO} by using the full HLN equation [58,59] (See Supplemental Material [46]). The extracted l_{SO} is much smaller compared to l_ϕ (as expected for TI systems) ruling out that possibility as well.

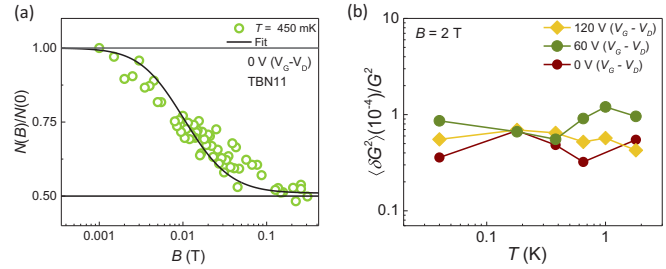

FIG. 4. Variation of magnitude of conductance fluctuations with magnetic field. (a) Normalized UCF magnitude at $V_G - V_D = 0$ V for 450 mK clearly exhibiting a factor of two reduction indicating the intrinsic preservation of time reversal symmetry in these systems. The solid line is a fit to the data according to Eq. (4). (b) Normalized variance $\delta G^2/G^2$ as a function of T for $B_\perp = 2$ T at $V_G - V_D = 0$, 60, and 120 V. The qualitative nature of saturation does not change even upon the application of a high magnetic-field, probably indicating that magnetic moments or surface-bulk coupling are not responsible for the saturation.

The most common reason, however, for the saturation of l_ϕ is the presence of magnetic impurities or localized spins, which leads to the saturation even in extremely pure systems [23,25,26]. Experimental and theoretical studies have reported the presence of localized spins [60] or intrinsic magnetic instabilities in the TI surface [61]. One manifestation of the presence of magnetic impurities can be long- or short-range magnetic ordering, which can lead to the removal of TRS in the system. To probe this, we have measured $\langle \delta G^2 \rangle$ as a function of $B_\perp$ on TBN11. The magnitude of the conductance fluctuations is plotted as $N_G(B)/N_G(0)$ ($N_G = \langle \delta G^2 \rangle / \langle G^2 \rangle$ is the normalized variance) in Fig. 4(a). We observe a factor of two reduction in the normalized magnitude when $B_\perp \gg B_\phi$ due to the suppression of the Cooperon contribution in transport and the crossover of the system from symplectic to unitary symmetry class, which indicates that TRS is intact intrinsically in these systems. For a quantitative understanding, the normalized magnitude has been fitted with the expression [17,35,37,62,63]

$$\begin{aligned} N(B)/N(0) &= \frac{1}{2} + \frac{1}{b^2} \sum_{n=0}^{\infty} \frac{1}{\left[\left(n + \frac{1}{2}\right) + \frac{1}{b}\right]^3} \\ &= \frac{1}{2} - \frac{1}{2b^2} \Psi'' \left(\frac{1}{2} + \frac{1}{b}\right). \end{aligned} \tag{4}$$

Here $b = 8\pi B (l_\phi)^2/(h/e)$, Ψ'' is the double derivative of the digamma function, and l_ϕ is the fitting parameter. The solid line in Fig. 4(a) is the fit according to Eq. (4), which captures the variation with normalized magnitude with B. The l_ϕ obtained from the fit is 200 nm, similar to l_ϕ obtained from UCF and MR, which confirms the validity of the analysis and the factor of two reduction.

Spin-flip scattering due to the presence of unwanted magnetic impurities, e.g., due to finite purity of the metal components, may also cause dephasing. To investigate this, we have extracted $\langle \delta G^2 \rangle$ as a function of T for $B_\perp = 2$ T for different $V_G - V_D$. The normalized magnitude $\langle \delta G^2 \rangle / G^2$ shows a saturation for $B_\perp = 2$ T for $T < 2$ K, as displayed in Fig. 4(b). The presence of a magnetic field $B_\perp \gg k_B T/(g\mu_B)$ is expected to freeze the magnetic moments and suppress spin-flip scattering in the sample. Here k_B, g, and μ_B are the Boltzmann constant, Landé g-factor, and Bohr magneton, respectively. The fact that the saturation persists even in the presence of $B_\perp$ indicates that it is not due to any magnetic impurities or localized spins in the system. To probe the effect of coupling between the surface states and charged disorders in the bulk, we have measured the conductance fluctuations for more positive gate voltages ($V_G - V_D = 60$ V and 120 V). The number density at $V_G - V_D = 120$ V is 8.6×10^{16} m^{-2}, which corresponds to bulk transport dominated regime, where the coupling of the two surfaces and the bulk is also higher, compared to that near the Dirac point (−60 V) [12,64]. However, the nature of saturation also does not change for more positive gate voltages, implying that it is independent of the coupling between surface states and the charged puddles in the bulk, similar to M10 [Fig. 3(c)].

III. DISCUSSIONS

While the exact source of saturation remains unascertained, we discuss some plausible mechanisms that may lead to the saturation of l_ϕ in TIs. The saturation can arise from the presence of two-level systems as has been explored in Refs. [65,66]. Such two-level systems can arise from the charge fluctuations in the bulk, which are known to be the dominant source of $1/f$ noise in TI [40–42]. The relaxation dynamics of these charged defects in the bulk can lead to a very weak dependence of l_ϕ on T. Liao *et al.* have shown that the charge puddles in the bulk lead to a sublinear dependence of l_ϕ on T [12]. It is possible that at low T, these uncompensated charges are strongly localized, leading to reduced screening of electromagnetic fluctuations. This can produce additional dephasing of the surface carriers, which might limit l_ϕ to a finite value. Recently Väyrynen *et al.* have proposed backscattering of electrons by electromagnetic fluctuations from the charge puddles in the bulk in 2D TIs [67]. The effect of such inelastic scattering on l_ϕ in 3D TIs remains to be seen and may also provide crucial insight into the factors leading to the saturation of l_ϕ in topological insulators. Novell *et al.* have demonstrated that short-range nonmagnetic impurities present near the edges, along with electron-electron interactions can act as magnetic scatterers in 2D TIs. The effect of such scatterings on l_ϕ in 3D-TIs may also shed some light on the saturation that has been observed [68].

In conclusion, we have measured the Fermi energy and time-dependent conductance fluctuations and magnetoresistance to probe the sources of dephasing of the surface carriers in topological insulators. The phase breaking length obtained from both of these techniques show a saturation below some specific temperatures which are sample dependent. We have eliminated several factors that may lead to the saturation of l_ϕ such as finite-size effects, spin-orbit coupling length, and surface-bulk coupling. The magnetic field dependence of the conductance fluctuations also eliminates the possibility of the saturation arising due to the presence of magnetic impurities or localized spins in the system. Our work suggests the presence of an additional dephasing mechanism in TIs which is dominant at low temperatures and limits the phase breaking length to a finite value at low temperatures.

ACKNOWLEDGMENTS

S.I., S.B., D.S., and A.G. acknowledge support from DST, India. A.R., A.K., and N.S. acknowledge support from The Pennsylvania State University Two-Dimensional Crystal Consortium – Materials Innovation Platform (2DCC-MIP), which is supported by NSF cooperative Agreement No. DMR-1539916.

S.I. and S.B. contributed equally to this work.

[1] M. Z. Hasan and C. L. Kane, Rev. Mod. Phys. **82**, 3045 (2010).
[2] J. E. Moore, Nature (London) **464**, 194 (2010).
[3] M. König, S. Wiedmann, C. Brüne, A. Roth, H. Buhmann, L. W. Molenkamp, X.-L. Qi, and S.-C. Zhang, Science **318**, 766 (2007).
[4] Y. Chen, J. G. Analytis, J.-H. Chu, Z. Liu, S.-K. Mo, X.-L. Qi, H. Zhang, D. Lu, X. Dai, and Z. Fang, Science **325**, 178 (2009).
[5] C.-Z. Chang, J. Zhang, X. Feng, J. Shen, Z. Zhang, M. Guo, K. Li, Y. Ou, P. Wei, and L.-L. Wang, Science **340**, 167 (2013).
[6] S. Islam, J. K. Mishra, A. Kumar, D. Chatterjee, N. Ravishankar, and A. Ghosh, Nanoscale **11**, 1579 (2019).
[7] Y. S. Kim, M. Brahlek, N. Bansal, E. Edrey, G. A. Kapilevich, K. Iida, M. Tanimura, Y. Horibe, S.-W. Cheong, and S. Oh, Phys. Rev. B **84**, 073109 (2011).
[8] R. Ockelmann, A. Müller, J. H. Hwang, S. Jafarpisheh, M. Drögeler, B. Beschoten, and C. Stampfer, Phys. Rev. B **92**, 085417 (2015).
[9] J. Wang, A. M. DaSilva, C.-Z. Chang, K. He, J. K. Jain, N. Samarth, X.-C. Ma, Q.-K. Xue, and M. H. W. Chan, Phys. Rev. B **83**, 245438 (2011).
[10] D. Zhang, A. Richardella, D. W. Rench, S.-Y. Xu, A. Kandala, T. C. Flanagan, H. Beidenkopf, A. L. Yeats, B. B. Buckley, P. V. Klimov, D. D. Awschalom, A. Yazdani, P. Schiffer, M. Z. Hasan, Z, and N. Samarth, Phys. Rev. B **86**, 205127 (2012).
[11] A. Kandala, A. Richardella, D. Zhang, T. C. Flanagan, and N. Samarth, Nano Lett. **13**, 2471 (2013).
[12] J. Liao, Y. Ou, H. Liu, K. He, X. Ma, Q.-K. Xue, and Y. Li, Nat. Commun. **8**, 16071 (2017).
[13] Z. Li, T. Chen, H. Pan, F. Song, B. Wang, J. Han, Y. Qin, X. Wang, R. Zhang, J. Wan *et al.*, Sci. Rep. **2**, 595 (2012).
[14] J. G. Checkelsky, Y. S. Hor, R. J. Cava, and N. P Ong, Phys. Rev. Lett. **106**, 196801 (2011).
[15] J.-J. Lin and J. Bird, J. Phys. Condens. Matter **14**, R501 (2002).

[16] H. Steinberg, J.-B. Laloë, V. Fatemi, J. S. Moodera, and P. Jarillo-Herrero, Phys. Rev. B **84**, 233101 (2011).

[17] S. Islam, S. Bhattacharyya, H. Nhalil, S. Elizabeth, and A. Ghosh, Phys. Rev. B **97**, 241412(R) (2018).

[18] Y. K. Fukai, S. Yamada, and H. Nakano, Appl. Phys. Lett. **56**, 2123 (1990).

[19] J. J. Lin and N. Giordano, Phys. Rev. B **35**, 1071 (1987).

[20] J. Vranken, C. Van Haesendonck, and Y. Bruynseraede, Phys. Rev. B **37**, 8502 (1988).

[21] P. Fournier, J. Higgins, H. Balci, E. Maiser, C. J. Lobb, and R. L Greene, Phys. Rev. B **62**, R11993(R) (2000).

[22] D. P. Pivin, Jr., A. Andresen, J. P. Bird, and D. K. Ferry, Phys. Rev. Lett. **82**, 4687 (1999).

[23] F. Schopfer, C. Bäuerle, W. Rabaud, and L. Saminadayar, Phys. Rev. Lett. **90**, 056801 (2003).

[24] P. Mohanty, E. M. Q. Jariwala, and R. A. Webb, Phys. Rev. Lett. **78**, 3366 (1997).

[25] F. Pierre and N. O. Birge, Phys. Rev. Lett. **89**, 206804 (2002).

[26] F. Pierre, A. B. Gougam, A. Anthore, H. Pothier, D. Esteve, and N. O. Birge, Phys. Rev. B **68**, 085413 (2003).

[27] P. Mohanty and R. A. Webb, Phys. Rev. B **55**, R13452 (1997).

[28] C. Chuang, L.-H. Lin, N. Aoki, T. Ouchi, A. M. Mahjoub, T.-P. Woo, R. K. Puddy, Y. Ochiai, C. Smith, and C.-T. Liang, Appl. Phys. Lett. **103**, 043117 (2013).

[29] B. Huard, A. Anthore, N. O. Birge, H. Pothier, and D. Esteve, Phys. Rev. Lett. **95**, 036802 (2005).

[30] S. Hikami, A. I. Larkin, and Y. Nagaoka, Prog. Theor. Phys. **63**, 707 (1980).

[31] N. O. Birge, B. Golding, and W. H. Haemmerle, Phys. Rev. B **42**, 2735 (1990).

[32] A. Ghosh and A. K. Raychaudhuri, Phys. Rev. Lett. **84**, 4681 (2000).

[33] A. Ghosh, S. Kar, A. Bid, and A. Raychaudhuri, arXiv:cond-mat/0402130.

[34] P. A. Lee and A. D. Stone, Phys. Rev. Lett. **55**, 1622 (1985).

[35] P. A. Lee, A. D. Stone, and H. Fukuyama, Phys. Rev. B **35**, 1039 (1987).

[36] A. N. Pal, V. Kochat, and A. Ghosh, Phys. Rev. Lett. **109**, 196601 (2012).

[37] S. Shamim, S. Mahapatra, G. Scappucci, W. Klesse, M. Simmons, and A. Ghosh, Sci. Rep. **7**, 46670 (2017).

[38] A. A. Taskin, Z. Ren, S. Sasaki, K. Segawa, and Y. Ando, Phys. Rev. Lett. **107**, 016801 (2011).

[39] C. R. Dean, A. F. Young, I. Meric, C. Lee, L. Wang, S. Sorgenfrei, K. Watanabe, T. Taniguchi, P. Kim, and K. L. Shepard, Nat. Nanotechnol. **5**, 722 (2010).

[40] S. Bhattacharyya, A. Kandala, A. Richardella, S. Islam, N. Samarth, and A. Ghosh, Appl. Phys. Lett. **108**, 082101 (2016).

[41] S. Islam, S. Bhattacharyya, A. Kandala, A. Richardella, N. Samarth, and A. Ghosh, Appl. Phys. Lett. **111**, 062107 (2017).

[42] S. Bhattacharyya, M. Banerjee, H. Nhalil, S. Islam, C. Dasgupta, S. Elizabeth, and A. Ghosh, ACS Nano **9**, 12529 (2015).

[43] L. Bao, L. He, N. Meyer, X. Kou, P. Zhang, Z.-G. Chen, A. V. Fedorov, J. Zou, T. M. Riedemann, and T. A. Lograsso, Sci. Rep. **2**, 726 (2012).

[44] S. Matsuo, T. Koyama, K. Shimamura, T. Arakawa, Y. Nishihara, D. Chiba, K. Kobayashi, T. Ono, C.-Z. Chang, K. He *et al.*, Phys. Rev. B **85**, 075440 (2012).

[45] S. Matsuo, K. Chida, D. Chiba, T. Ono, K. Slevin, K. Kobayashi, T. Ohtsuki, C.-Z. Chang, K. He, X.-C. Ma *et al.*, Phys. Rev. B **88**, 155438 (2013).

[46] See Supplemental Material at http://link.aps.org/supplemental/10.1103/PhysRevB.99.245407 for α from HLN equation, Electron temperature calibration, Estimation of spin-orbit coupling length.

[47] R. V. Gorbachev, F. V. Tikhonenko, A. S. Mayorov, D. W. Horsell, and A. K. Savchenko, Phys. Rev. Lett. **98**, 176805 (2007).

[48] J. H. Scofield, Rev. Sci. Instrum. **58**, 985 (1987).

[49] N. O. Birge, B. Golding, and W. H. Haemmerle, Phys. Rev. Lett. **62**, 195 (1989).

[50] A. Trionfi, S. Lee, and D. Natelson, Phys. Rev. B **70**, 041304(R) (2004).

[51] R. Koushik, S. Kumar, K. R. Amin, M. Mondal, J. Jesudasan, A. Bid, P. Raychaudhuri, and A. Ghosh, Phys. Rev. Lett. **111**, 197001 (2013).

[52] E. Akkermans and G. Montambaux, *Mesoscopic physics of electrons and photons* (Cambridge University Press, Cambridge, 2007).

[53] P. Adroguer, D. Carpentier, J. Cayssol, and E. Orignac, New J. Phys. **14**, 103027 (2012).

[54] C. Beenakker and H. van Houten, in *Solid State Phys.*, Vol. 44 (Elsevier, 1991), pp. 1–228.

[55] S. V. Morozov, K. S. Novoselov, M. I. Katsnelson, F. Schedin, L. A. Ponomarenko, D. Jiang, and A. K. Geim, Phys. Rev. Lett. **97**, 016801 (2006).

[56] X. Wu, X. Li, Z. Song, C. Berger, and W. A. de Heer, Phys. Rev. Lett. **98**, 136801 (2007).

[57] M. Liu, C.-Z. Chang, Z. Zhang, Y. Zhang, W. Ruan, K. He, L.-l. Wang, X. Chen, J.-F. Jia, S.-C. Zhang, O. K. Xue, X. Ma, Y. Wang *et al.*, Phys. Rev. B **83**, 165440 (2011).

[58] S. Zhang, R. McDonald, A. Shekhter, Z. Bi, Y. Li, Q. Jia, and S. T. Picraux, Appl. Phys. Lett. **101**, 202403 (2012).

[59] R. Dey, T. Pramanik, A. Roy, A. Rai, S. Guchhait, S. Sonde, H. C. Movva, L. Colombo, L. F. Register, and S. K. Banerjee, Appl. Phys. Lett. **104**, 223111 (2014).

[60] D. M Nisson, A. P. Dioguardi, P. Klavins, C. H. Lin, K. Shirer, A. C. Shockley, J. Crocker, and N. J. Curro, Phys. Rev. B **87**, 195202 (2013).

[61] Y. Baum and A. Stern, Phys. Rev. B **85**, 121105 (R) (2012).

[62] A. D. Stone, Phys. Rev. B **39**, 10736 (1989).

[63] S. Shamim, B. Weber, D. W. Thompson, M. Y. Simmons, and A. Ghosh, Nano Lett. **16**, 5779 (2016).

[64] D. Kim, S. Cho, N. P. Butch, P. Syers, K. Kirshenbaum, S. Adam, J. Paglione, and M. S. Fuhrer, Nat. Phys. **8**, 459 (2012).

[65] Y. Imry, H. Fukuyama, and P. Schwab, Europhys. Lett. **47**, 608 (1999).

[66] A. N. Aleshin, V. I. Kozub, D.-S. Suh, and Y. W. Park, Phys. Rev. B **64**, 224208 (2001).

[67] J. I. Väyrynen, D. I. Pikulin, and J. Alicea, Phys. Rev. Lett. **121**, 106601 (2018).

[68] P. Novelli, F. Taddei, A. K. Geim, and M. Polini, Phys. Rev. Lett. **122**, 016601 (2019).